Arabian Journal of Chemistry (2017) **10**, 708–714

King Saud University

Arabian Journal of Chemistry

www.ksu.edu.sa
www.sciencedirect.com

ORIGINAL ARTICLE

Probing the molecular orientation of chemically polymerized polythiophene-polyrotaxane via solid state NMR

Mujeeb Khan [a,d,*], **Gunther Brunklaus** [b,d], **Shahzada Ahmad** [c,d]

[a] *Department of Chemistry, College of Science, King Saud University, P.O. Box 2455, Riyadh 11451, Saudi Arabia*
[b] *Westfälische Wilhelms-Universität, Institut für Physikalische Chemie, D-48149 Münster, Germany*
[c] *Abengoa Research, C/Energía Solar n° 1, Campus Palmas Altas, 41014 Sevilla, Spain*
[d] *Max Planck Institute for Polymer Research, P.O. Box 3148, D-55021 Mainz, Germany*

Received 20 October 2016; accepted 6 January 2017
Available online 16 January 2017

KEYWORDS

Polythiophene;
Polyrotaxanes;
Thiophene [2]Rotaxane;
Solid-state NMR

Abstract Polyrotaxanes have attracted significant attention of scientific community and are being explored towing to its electro-optical properties. The orientation and the molecular structure of polyrotaxanes influence its final properties. Thus a, detail understanding of the structure of such compounds at the molecular level will provide an opportunity to further tune and optimize their properties. Here chemically polymerized polythiophene polyrotaxane i.e. Thiophene [2]Rotaxane which is the rotaxane like compound consisting of several macrocycle, was studied in the powdered form. This allowed us to investigate the molecular structure of polyrotaxane and to obtain the detail insights into its structure property relationship via solid state NMR. The as-obtained polymer has also been characterized via various other techniques including UV spectroscopy, solution NMR and so on. We elucidated the structure of the Thiophene [2]Rotaxane monomer remained intact even after polymerization.

1. Introduction

Polythiophenes are one of the most promising (semi)conducting materials for organic electronics, owing to its application in many devices such as organic field-effect transistors (OFET), organic light-emitting diode (OLED), photo-voltaic materials or electrochromic materials. This has gained momentum due to the ease of flexibility and rather simple processability of this type of materials (Osaka and McCullough, 2008; McCullough, 1998; Gohier et al., 2013; Zhang et al., 2011; Yaman et al., 2014; Irimia-Vladu, 2014; Shao et al., 2013). Sincere efforts are devoted to investigate insulated molecular wires in which conducting polymers are wrapped with insulating substituents or macrocyclic compounds (Li and Shi, 2013; Jeong et al.,

* Corresponding author at: Department of Chemistry, College of Science, King Saud University, P.O. Box 2455, Riyadh 11451, Saudi Arabia.
E-mail address: kmujeeb@ksu.edu.sa (M. Khan).
Peer review under responsibility of King Saud University.

Production and hosting by Elsevier

http://dx.doi.org/10.1016/j.arabjc.2017.01.003
1878-5352

2012). The insulating layer suppress strong molecular and electronic interactions between the conductive polymers, which results in better solubility in the organic solvents and higher quantum yield of the fluorescence emission (Zhou et al., 2006; Kuo et al., 2013; Cochran et al., 2013). Notably, such insulated molecular wires comprised of tetracationic cyclophanes cyclobis(paraquat-p-phenylene)s (CBPQT4+s) and polythiophene (Fig. 1) were recently introduced (Ikeda et al., 2009).

In addition, thin layers of insulated molecular wires on electrode surfaces obtained through electrochemical polymerization of the thiophene [2]Rotaxane were described (Ikeda et al., 2011). The [*n*]rotaxane is the compound consisting of the macrocycle topologically entrapped by the dumbbell-shaped molecule. Here the number *n* in the square bracket indicates the number of the units (macrocycle and dumbbell-shaped compound) in the rotaxane compound (Yildiz et al., 2008). Polyrotaxanes are rotaxane-like compounds consisting of many macrocycles and dumb bell-shaped moieties and thus were dubbed "polythiophene polyrotaxanes" (Ikeda et al., 2009). In this work, we report the structure and characterization of polythiophene polyrotaxanes obtained from chemical polymerization of the thiophene [2]Rotaxane. The main aim of this study was to investigate the nature of the orientation of the macrocycle within the compound and its impact on the physicochemical properties, unraveling the corresponding structure property relationship via solid state NMR while putting forward the definition of rotaxane molecules. In particular, the powdered samples merely derived from chemical polymerization provided the opportunity to analyze its properties in more realistic ways. All as-prepared samples were further characterized by solution NMR, and their preliminary charge transport properties were estimated from conductivity measurements and localized level properties.

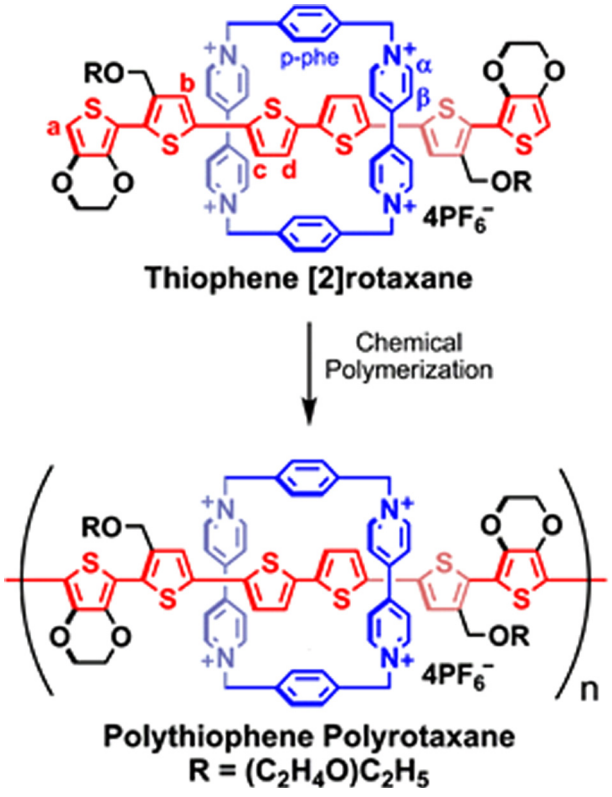

Fig. 1 Schematic illustration of the chemical polymerization of thiophene [2]Rotaxane to polythiophene polyrotaxane.

2. Materials and methods

2.1. Materials used

The thiophene [2]Rotaxane was synthesized according to a previous report (Ikeda et al., 2009). The chemical oxidant nitrosonium hexafluorophosphate ($NOPF_6$) was purchased from Acros Organics. The other chemicals and solvents were obtained from commercial sources and used as received. UV/Vis spectra were recorded at room temperature on a UV-2550 UV–Visible spectrophotometer (Shimadzu Co.). ^1H NMR spectra were recorded at room temperature on an Avance 250 FT NMR system (Bruker) with residual solvent as the internal standard. Acetonitirile (MeCN) and methyl alcohol (MeOH) were purchased from Sigma Aldrich.

2.2. Chemical polymerization of thiophene [2]Rotaxane

The thiophene [2]Rotaxane (25 mg, 1.2×10^{-5} mol) was dissolved in dry MeCN (0.4 mL). The solution was cooled to −10 °C with an ice bath. $NOPF_6$ (260 mg, 1.5 mmol) was dissolved in dry MeCN (5 mL). The $NOPF_6$ solution (0.20 mL) was added to the thiophene [2]Rotaxane solution. The reaction mixture was stirred at −10 °C for five minutes. After adding pyridine (1 mL) to reduce the product, the solution was diluted by acetone (5 mL). The solution was added dropwise to 2 N NH_4PF_6 aqueous solution (100 mL) to precipitate the product. The product was recovered by filtration and washed by dichloromethane (DCM). Subsequently the solid product was dissolved in acetone again and added dropwise in MeOH (100 mL) to precipitate the product. The product was recovered by filtration and dissolved in acetone again and then the solution was transferred to small flask and the solvent was removed by evaporation. Finally the product was dried under reduced pressure to afford deep red purple solid. [Yield: 22 mg (88%)].

2.3. Characterization

2.3.1. Solid-state NMR

Proton solid-state single-pulse and double-quantum (DQ) magic-angle spinning (MAS) (^1H, 850.1 MHz) as well as carbon cross-polarization (CP) and heteronuclear correlation (HETCOR) MAS NMR spectra (^{13}C, 213.8 MHz) were recorded at a 20 T magnet equipped with a Bruker Avance III console. Additional nitrogen CPMAS spectra (^{15}N, 30.4 MHz) were recorded at a Bruker Avance II 300 machine. All experiments were carried out at room temperature using commercially available Bruker 2.5 mm or 4 mm double-resonance MAS probes, respectively, at spinning frequencies of either 30 kHz or 5 kHz. Typical π/2-pulse lengths were adjusted to 2.5 μs (corresponding to B_1-fields of 100 kHz) and recycle delays of 15 s. The ^1H and ^{13}C MAS NMR spectra were referenced with respect to tetramethylsilane (TMS) using solid adamantane as secondary standard (1.84 ppm for ^1H and 29.456 ppm for ^{13}C); ^{15}N spectra were referenced with respect to solid $^{15}NH_4Cl$ (−341.0 ppm). The back-to-back (BaBa) (Geen et al., 1994; Gottwald et al., 1995; Sommer et al., 1995; Feikeet al., 1996; Saalwächter et al., 1999; Saalwächter et al., 2001) recoupling sequence was used to excite and reconvert double-quantum coherences, applying States-TPPI (Marion et al., 1989) for phase sensitive detection.

2.3.2. Conductivity measurements

Conductivity measurements were made using pellets of the samples (thickness = 0.6 mm, diameter: 5 mm) and a Solartron 1260 impedance gain phase analyzer in a frequency range of 0.1 Hz to 10^6 Hz. The sample was scanned in the temperature range of 0–100 °C, at an interval of 10 min where the temperature was stabilized at every step for 10 min. 100 mM solution of rotaxane molecule in DMSO was spin-coated on a Platinum coated silicon wafer at 2000 rpm for 30 s followed by annealing for 30 min at 60 °C. Conductive scanning force microscopy (CSFM) measurements were performed in contact mode by Torsional resonance tunneling AFM (TR TUNA) (Veeco) extended with current amplifier module for current measurement. For CSFM the Pt/Ir coating conductive probes PPP-EFM (Nanosensors) were used. The operating range for the current amplifier was set to 20 pA to cover all currents at bias voltages of 50 mV. The sample was glued with silver paste on a conductive steel substrate and to avoid electromagnetic noise, the scanner was shielded by wrapping Al foil around the SFM recording setup. In order to minimize possible destruction to the surface, minimum possible force was applied to record the surface topography.

3. Results and discussion

3.1. Preparation of polythiophene polyrotaxane

The earlier reported polythiophene polyrotaxane was insoluble in variety of solvents (Ikeda et al., 2009) whereas the powdered sample obtained by chemical polymerization in this study has shown significant enhancement in its solubility and is soluble in variety of organic solvents including MeCN, DMF and DMSO, respectively. Polythiophene polyrotaxane is a polyelectrolyte, and thus the counter ion of $CBPQT^{4+}$ holds the key to control the solubility. The counter ions in this and previous studies were chosen as PF_6^- or ClO_4^-, where PF_6^- is known to be hydrophobic compared to ClO_4^-.

Fig. 2 shows ^{1}H NMR spectra of the thiophene [2]Rotaxane and polythiophene polyrotaxane (in solution). After the polymerization, it is evident that the signal attributed to side chain methylene protons of the polythiophene is broadened while the peak reflecting thiophene aromatic protons disappeared, most likely due to longer spin lattice relaxation time of the protons based on reduced mobility of the polythiophene chain.

The ^{1}H signal of methylene protons of the 3,4-ethylenedioxythiophene (EDOT) unit shift to lower magnetic field after the polymerization, in good agreement with previous data (Ikeda et al., 2009, 2011). EDOT units transform to dimeric bis(3,4-ethylenedioxythiophene) (BEDOT) moieties upon polymerization so that remaining EDOT methylene protons are affected by stronger anisotropic deshielding effects from the formed BEDOT units. In order to rule out the possibility that the polythiophene decomposes after the polymerization, we conducted an UV–Vis absorption measurement. Fig. 3 shows UV–Vis spectrum of (a) thiophene [2]Rotaxane and (b) polythiophene polyrotaxane. The peaks at 260 nm correspond to the absorption of $CBPQT^{4+}$ and it clearly shows the shifting of absorption peaks of the (π-π^*) band to longer wavelength after polymerization (436 nm → 514 nm) indicating expansion of π-conjugation. It is worth mentioning that the intensity of the (π-π^*) band does not decrease upon polymerization, clearly reflecting that thiophene units are not decomposed after polymerization. In spite of our best possible efforts to establish the corresponding molecular weight of the polythiophene polyrotaxane, analysis via size exclusion chromatography was not feasible, particularly to avoid deterioration of the column due to adsorbed polyelectrolyte sample on the column resin.

3.2. Solid-state NMR

At first, we acquired the corresponding ^{1}H MAS NMR spectra of both thiophene [2]Rotaxane and polythiophene polyrotaxane, yielding quite comparable spectra with resonances centered at 8.8 ppm, around 7.5–7.7 ppm, 3.5 ppm and 0.8 ppm, respectively, except for the peaks at 5.3–5.8 ppm, which exhibit rather pronounced intensities in case of polythiophene polyrotaxane (cf. Fig. 4). In order to simplify an assignment of the peaks, we also considered the ^{1}H MAS NMR spectrum of $CBPQT^{4+}$ where three peaks at 8.3 ppm, 7.6 ppm and 5.3 ppm could be observed (data not shown). Based on available solution NMR data, the latter peak can be attributed to the methylene bridging units of $CBPQT^{4+}$ while the peak at 8.3 ppm likely reflects the β-protons (Fig. 1), rendering the p-phe and α-protons at about 7.6 ppm. Successful wrapping of $CBPQT^{4+}$ around the thiophene backbone (at first glance) should not lead to significant shifts of the $CBPQT^{4+}$ proton resonances, and additional resonances at about 3.5 and 0.8 ppm merely indicate OCH_2 moieties of the ethylene glycol

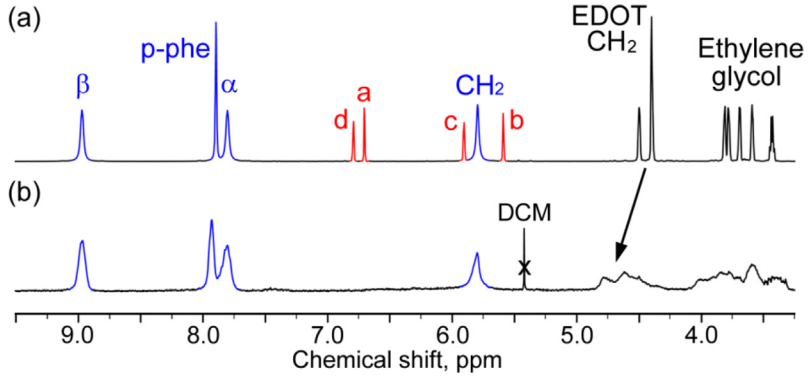

Fig. 2 ^{1}H solution NMR spectra of (a) thiophene [2]Rotaxane and (b) polythiophene polyrotaxane.

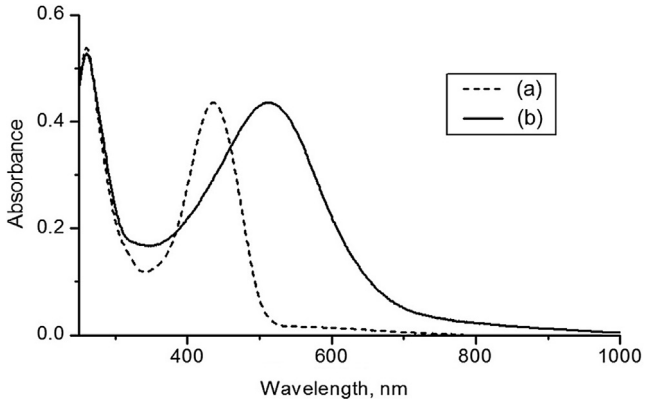

Fig. 3 UV-vis absorption spectra of (a) thiophene [2]Rotaxane and (b) polythiophene polyrotaxane.

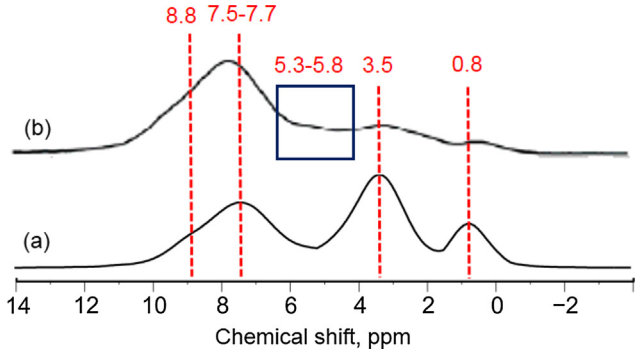

Fig. 4 ^{1}H MAS NMR spectra of both (a) thiophene [2]Rotaxane and (b) polythiophene polyrotaxane

side chains while the peaks representing the EDOT-CH_2 and aromatic protons of the (poly-) thiophene cannot be unambiguously identified.

In addition, we considered ^{13}C-CPMAS NMR spectra of the compounds (Fig. 5), which revealed very similar environments in thiophene [2]Rotaxane and polythiophene polyrotaxane, respectively. Note that the ^{13}C peak around 100 ppm

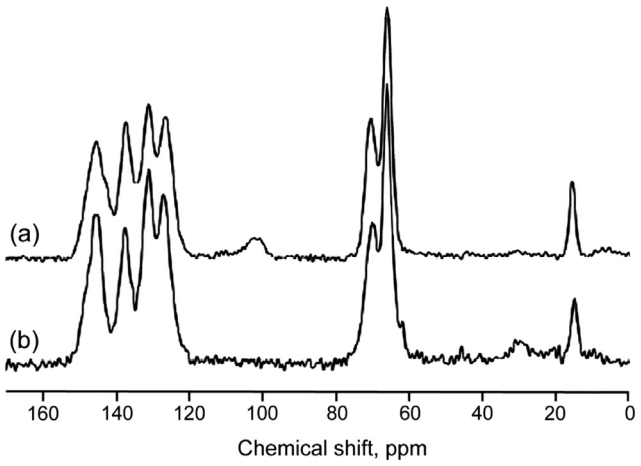

Fig. 5 ^{13}C-CPMAS NMR spectra of (a) thiophene [2]Rotaxane and (b) polythiophene polyrotaxane

corresponds to the aromatic carbons of the EDOT end units of the sexithiophene moiety, which upon successful polymerization is very likely shifted to another spectral region or may not be detectable due to negligible intensity. Signals attributable to either sexithiophene or polythiophene backbone are well established in the region between 120 and 140 ppm (Barbarella et al., 1996; Khan et al., 2008) hence overlapping with most ^{13}C NMR signals from $CBPQT^{4+}$ units (data not shown), except for the aromatic carbons corresponding to the α-proton, β-proton and the p-phe moieties, which resonate at 150.4 ppm, 146.3 ppm and 144.2 ppm, respectively. The OCH_2 carbons from the ethylene glycol side chain as well as the EDOT units are identified at 65.2 and 69.6 ppm, while the methyl end groups resonate at 14.7 ppm. In addition, the ^{15}N-CPMAS spectra of thiophene [2]Rotaxane and polythiophene polyrotaxane both exhibit a single peak at around −160 ppm (data not shown) thereby indicating that the chemical structure of the $CBPQT^{4+}$ units is preserved upon polymerization.

Insight into the local packing and spatial proximity of building units can be in principle obtained from the analysis of both homo- and heteronuclear dipolar correlation (HETCOR) spectra, such as 2D ^{1}H-^{1}H double-quantum (DQ) (Brown, 2007) and ^{1}H-^{13}C CP-HETCOR MAS NMR spectra (Cook, 2004). In the former case, couplings among like spins result in characteristic diagonal peaks while couplings of unlike spins are reflected by the presence of cross peaks (Brown and Spiess, 2001). Depending on the strength of the underlying dipolar coupling trivial DQ peaks merely reflecting the molecular structure of the constituents can be in principle distinguished from cross peaks that result from a particular spatial packing (Khan et al., 2010).

Both the polythiophene backbone and the macrocycle ($CBPQT^{4+}$), however, contain aromatic and aliphatic protons with similar ^{1}H chemical shifts thus rendering an unambiguous assignment of the observed DQ cross-peaks in case of the polythiophene polyrotaxane rather difficult. Nevertheless, for the sexithiophene rotaxane, the DQ cross-peak among the protons at 7.6 ppm (attributed to the p-phe and α-protons of $CBPQT^{4+}$) and the methyl groups of ethylene oxide side chains at 0.8 ppm strongly suggest that the macrocycle is entrapped by the dumbbell-shaped sexithiophene (Fig. 6). Note that the corresponding ^{1}H-^{13}C CP-HETCOR MAS NMR spectra of both thiophene [2]Rotaxane (Supp. Info) and polythiophene polyrotaxane (Cf. Fig. 7) are almost indistinguishable, thus rendering it very reasonable that the polythiophene backbone is also encapsulated by $CBPQT^{4+}$ macrocycles.

3.3. Conductivity measurement

Fig. 8 shows an Arrhenius-type plot of conductivity for the polythiophene polyrotaxane. The conductivity increases gradually with the increase in temperature while in the cooling curve a straight line is observed. The exponential increase in the electronic conductivity with (1/T) is in agreement with semiconductor behavior, since the number of charge carriers increases (Yuen et al., 2011). The activation energy obtained from best fit in the cooling curve amounts to 0.43 eV for the pristine sample while after iodine doping, it attained a value of 0.21 eV. Notably, the rather high activation energy

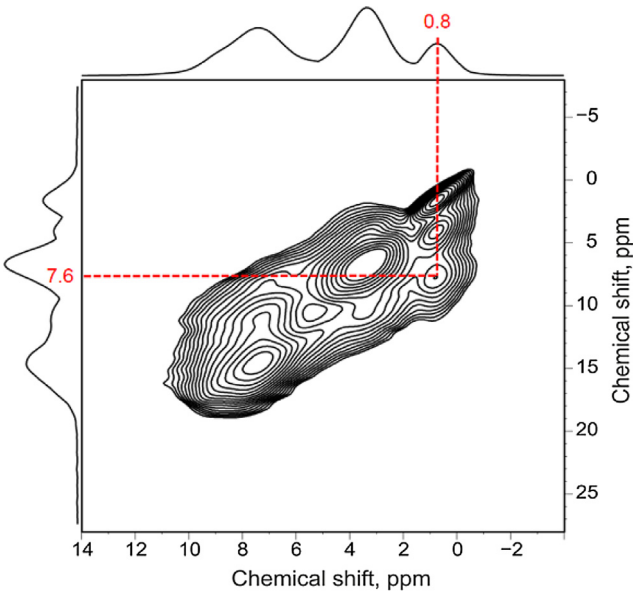

Fig. 6 2D ^{1}H-^{1}H double-quantum (DQ) MAS NMR spectrum of thiophene [2]Rotaxane. 2D ^{1}H-^{1}H double-quantum spectrum of polythiophene polyrotaxane is provided in SI.

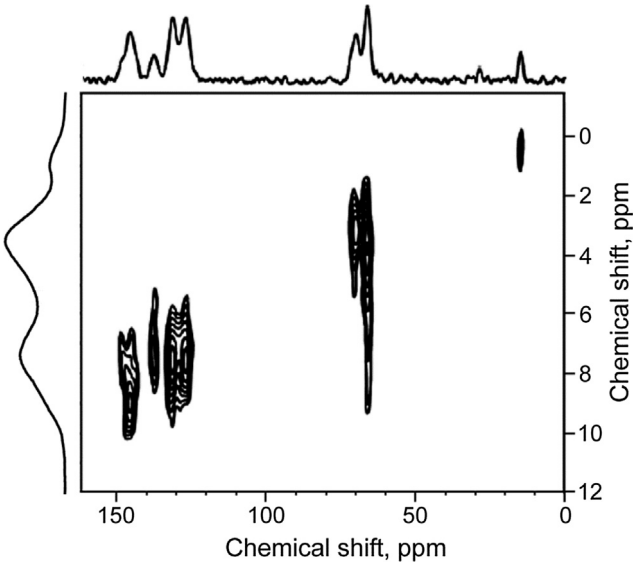

Fig. 7 ^{1}H-^{13}C CP-HETCOR MAS NMR spectrum of polythiophene polyrotaxane. ^{1}H-^{13}C CP-HETCOR MAS NMR spectrum of thiophene [2]Rotaxane is provided in SI.

corresponds to a relatively low conductivity; the slope of the curve follows a linear behavior thus suggesting that a small amount of energy is required to facilitate a hopping of the electrons. The observable electronic conductivity changed two orders of magnitude within the considered temperature range, illustrating a thermally activated process.

The electronic conductivities were in the range of $>10^{-10}$ S/cm at 80 °C and up to $>10^{-8}$ S/cm at higher temperatures (150 °C). After doping (for which the sample was exposed to iodine vapor for 15 min), we observed a significantly enhanced conductivity at low temperature while at

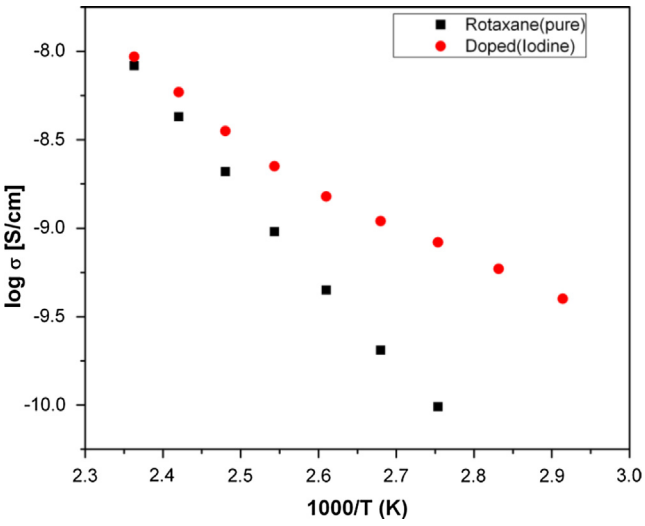

Fig. 8 Arrhenius plot of conductivity for the polythiophene polyrotaxane

higher temperature it remained fairly constant. The preliminary data suggest that these polythiophene polyrotaxanes constitute less effective electronic conductors, possibly due to partial suppression of the electron hopping between the polymer chains.

The surface roughness of the film was checked by SFM and the root mean square (RMS) roughness of films was 2.2 nm (scan size 2.5×2.5 μm^2). We have found that the surface was much smoother than that prepared by electrochemical polymerization (RMS roughness: 4.8 nm). Conductive scanning force microscopy was carried out to check the current homogeneities at nanometer-scale level, (Yoon et al., 2011) and it allows to simultaneously measure topography and current images. The current mapping is the flow of local current between the probe and sample under constant applied vias (E). Fig. 9 shows the current images of the polythiophene polyrotaxane film. The current image shows the inhomogeneity of the conductance in the film, probably due to the inhomogeneous molecular packing on the film. The average RMS current intensity is 2.3 nA at $E = 500$ mV (Fig. 7a) while it rises to 4.7 nA at $E = 1000$ mV. The observable increase in the current intensity at higher voltage arises from the sum of two effects, the ohmic law of the current-potential relationship and the conductivity change upon doping (oxidation).

4. Conclusion

[n]Rotaxanes comprise an important class of compounds, which are entrapped with dumbbell-shaped macrocycles that have significant effects on their electro-optical properties. Chemically polymerized polythiophene polyrotaxane was obtained in powdered form and showed excellent solubility in various organic solvents. Nevertheless, to determine their molecular structure and orientation of constituents within such compounds in the solid state, advanced characterization techniques are required. Since in the considered case the powdered sample could be produced in good yield, we performed solid state NMR experiments. Though often strong

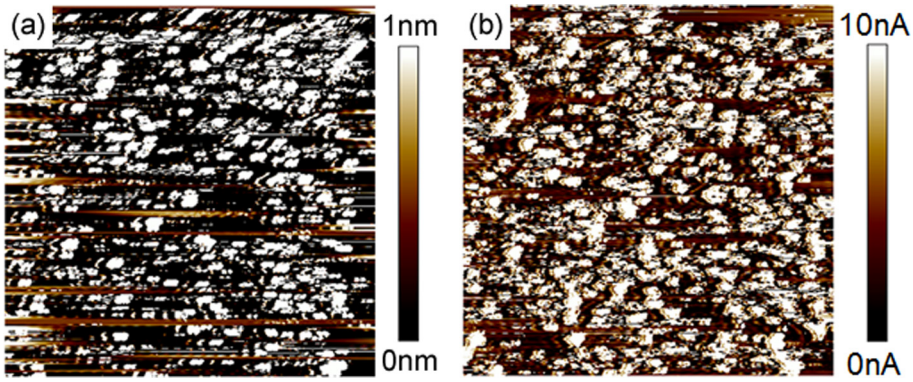

Fig. 9 AFM images of the polythiophene polyrotaxane film

homonuclear dipolar couplings among abundant protons lead to substantial line broadening in the ^{1}H MAS NMR spectra, high-resolution solid-state ^{1}H MAS NMR spectra could be obtained employing the so-called homonuclear dipolar decoupling sequences at ultra-fast MAS and rather high magnetic fields (850.1 MHz NMR), exploiting that the spectral resolution scales linearly with the applied magnetic field strength, while the ^{1}H–^{1}H dipolar interactions not only remain constant but also offer spectral filtering based on spin pair interactions. This study provided details of the molecular structure of the as-prepared polymer, where a comparative analysis of both monomer and polymer has revealed structural changes occurring upon polymerization. Though the thiophene moieties remained intact within the polymer, partially impaired electron hopping among polymer chains resulted in lesser electronic conductivity than anticipated for this type of compound. Note that solid state NMR constitutes an exceedingly important tool for the structure determination of powdered materials (including polymers) as well as analysis of molecular-level mobility, but still has some limitations in determining long ranged order. However, the rapidly evolving field of 'NMR crystallography' (which denotes a combination of the complementary techniques of solid-state NMR, powder diffraction and computational chemistry) offers great potential for in-depth characterization of polycrystalline or structurally less-defined powdered materials (Luedeker and Brunklaus, 2015; Luedeker et al., 2016). While diffraction experiments reveal topological data, solid-state NMR unravels connections, distances and orientation relations of constituents on more localized or intermediate length scales, that when complemented with molecular modeling and quantum chemical simulations allow to either verify existing structural models or even create novel meaningful structures, which may be highly beneficial in future work on polythiophene polyrotaxanes.

Acknowledgments

This project was supported by King Saud University, Deanship of Scientific Research, College of Science, Research Center.

The sample of the thiophene [2]rotaxanes was kindly supplied from Dr. T. Ikeda.

Appendix A. Supplementary material

Supplementary data associated with this article can be found, in the online version, at http://dx.doi.org/10.1016/j.arabjc.2017.01.003.

References

Barbarella, G., Casarini, D., Zambianchi, M., Favaretto, L., Rossini, S., 1996. ^{13}C CPMAS NMR characterization and molecular dynamics of oligothiophenes in the solid state. Adv. Mater. 8, 69–73.

Brown, S.P., 2007. Probing proton–proton proximities in the solid state. Progr. Nucl. Magn. Reson. Spectros. 50, 199–251.

Brown, S.P., Spiess, H.W., 2001. Advanced solid-state NMR methods for the elucidation of structure and dynamics of molecular, macromolecular, and supramolecular systems. Chem. Rev. 101, 4125–4155.

Cochran, J.E., Amir, E., Sivanandan, K., Ku, S.Y., Seo, J.H., Collins, B.A., Tumbleston, J.R., Toney, M.F., Ade, H., Hawker, C.J., 2013. J. Poly. Sci. B: Poly. Phys. 51, 48–56.

Cook, R.L., 2004. Coupling nmr to nom. Anal. Bioanal. Chem. 378, 1484–1503.

Feike, M., Demco, D.E., Graf, R., Gottwald, J., Hafner, S., Spiess, H. W., 1996. Broadband multiple-quantum NMR spectroscopy. J. Magn. Reson. A122, 214–221.

Geen, J., Titman, J., Gottwald, J., Spiess, H.W., 1994. Solid-state proton multiple-quantum NMR spectroscopy with fast magic angle spinning. Chem. Phys. Lett. 227, 79–86.

Gohier, F.D.R., Frère, J., Roncali, P., 2013. 3-Fluoro-4-hexylthiophene as a Building Block for Tuning the Electronic Properties of Conjugated Polythiophenes. J. Org. Chem. 78, 1497–1503.

Gottwald, J., Demco, D.E., Graf, R., Spiess, H.W., 1995. High-resolution double-quantum NMR spectroscopy of homonuclear spin pairs and proton connectivities in solids. Chem. Phys. Lett. 243, 314–323.

Ikeda, T., Higuchi, M., Kurth, D.G., 2009. From thiophene [2] Rotaxane to polythiophene polyrotaxane. J. Am. Chem. Soc. 131, 9158–9159.

Ikeda, T., Higuchi, M., 2011. Synthesis of thiophene-capped [2] Rotaxanes. Tetrahedron 67, 3046–3052.

Irimia-Vladu, M., 2014. "Green" electronics: biodegradable and biocompatible materials and devices for sustainable future. Chem. Soc. Rev. 43, 588–610.

Jeong, D.-C., Lee, H., Yang, K.S., Song, C., 2012. Effects of substituent on binaphthyl hinge-containing conductive polymers. Macromolecules 45, 9571–9578.

Khan, M., Enkelmann, V., Brunklaus, G., 2010. Crystal engineering of pharmaceutical co-crystals: application of methyl paraben as molecular hook. J. Am. Chem. Soc. 132, 5254–5263.

Khan, M., Brunklaus, G., Enkelmann, V., Spiess, H.-W., 2008. Transient states in [2+ 2] photodimerization of cinnamic acid: correlation of solid-state NMR and X-ray analysis. J. Am. Chem. Soc. 130, 1741–1748.

Kuo, C.-Y., Huang, Y.-C., Hsiow, C.-Y., Yang, Y.-W., Huang, C.-I., Rwei, S.-P., Wang, H.-L., Wang, L., 2013. Effect of side-chain architecture on the optical and crystalline properties of two-dimensional polythiophenes. Macromolecules 46, 5985–5997.

Li, C., Shi, G., 2013. Polythiophene-based optical sensors for small molecules. ACS Appl. Mater. Interfaces 5, 4503–4510.

Luedeker, D., Brunklaus, G., 2015. NMR crystallography of ezetimibe co-crystals. Solid State Nucl Mag. Res. 65, 29–40.

Luedeker, D., Gossmann, R., Langer, K., Brunklaus, G., 2016. Crystal engineering of pharmaceutical co-crystals: "NMR Crystallography" of niclosamide co-crystals. Cryst. Growth Des. 16, 3087–3100.

Marion, D., Ikura, M., Tschudin, R., Bax, A., 1989. Rapid recording of 2D NMR spectra without phase cycling. Application to the study of hydrogen exchange in proteins. J. Magn. Reson. 85, 393–399.

McCullough, R.D., 1998. The chemistry of conducting polythiophenes. Adv. Mater. 10, 93–116.

Osaka, I., McCullough, R.D., 2008. Advances in molecular design and synthesis of regioregular polythiophenes. Acc. Chem. Res. 41, 1202–1214.

Saalwächter, K., Graf, R., Spiess, H.W., 1999. Recoupled polarization transfer heteronuclear ^{1}H–^{13}C multiple-quantum correlation in solids under ultra-fast MAS. J. Magn. Reson. 140, 471–476.

Saalwächter, K., Graf, R., Spiess, H.W., 2001. Recoupled polarization-transfer methods for solid-state ^{1}H–^{13}C heteronuclear correlation in the limit of fast MAS. J. Magn. Reson. 148, 398–418.

Shao, M., He, Y., Hong, K., Rouleau, C.M., Geohegan, D.B., Xiao, K., 2013. A water-soluble polythiophene for organic field-effect transistors. Poly. Chem. 4, 5270–5274.

Sommer, W., Gottwald, J., Demco, D.E., Spiess, H.W., 1995. Dipolar heteronuclear multiple-quantum NMR spectroscopy in rotating solids. J. Magn. Reson. A 113, 131–134.

Yaman, B., Terkesli, I., Turksoy, K., Sanyal, A., Mutlu, S., 2014. Fabrication of a planar water gated organic field effect transistor using a hydrophilic polythiophene for improved digital inverter performance. Org. Electron. 15, 646–653.

Yoon, J.A., Kamada, J., Koynov, K., Mohin, J., Nicolaÿ, R., Zhang, Y., Balazs, A.C., Kowalewski, T., Matyjaszewski, K., 2011. Self-healing polymer films based on thiol–disulfide exchange reactions and self-healing kinetics measured using atomic force microscopy. Macromolecules 45, 142–149.

Yildiz, E., Camurlu, P., Tanyeli, C., Akhmedov, I., Toppare, L., 2008. Soluble conducting polymer of 4-(2,5-di(thiophen-2-yl)-1H-pyrrol-1-yl)benzenamine and its multichromic copolymer with EDOT. J. Electroanal. Chem. 612, 247–256.

Yuen, J.D., Fan, J., Seifter, J., Lim, B., Hufschmid, R., Heeger, A.J., Wudl, F., 2011. High performance weak donor-acceptor polymers in thin film transistors: effect of the acceptor on electronic properties, ambipolar conductivity, mobility, and thermal stability. J. Am. Chem. Soc. 133, 20799–20807.

Zhang, Z.-G., Zhang, S., Min, J., Chui, C., Zhang, J., Zhang, M., Li, Y., 2011. Conjugated side-chain isolated polythiophene: synthesis and photovoltaic application. Macromolecules 45, 113–118.

Zhou, E., Tan, Z.A., Huo, L., He, Y., Yang, C., Li, Y., 2006. Effect of branched conjugation structure on the optical, electrochemical, hole mobility, and photovoltaic properties of polythiophenes. J. Phys. Chem. B 110, 26062–26067.